Direct Observation of Charge Transfer in Double-Perovskite-Like $RbMn[Fe(CN)_6]$

K. Kato
JASRI/SPring-8, 1-1-1 Kouto, Mikazuki-cho, Sayo-gun, Hyogo 679-5198, Japan

Y. Moritomo
Department of Applied Physics, Nagoya University, Nagoya 464-8603, Japan, and PRESTO. JST, 4-1-8 Honcho, Kawaguchi, Saitama 332-0012, Japan

M. Takata
JASRI/SPring-8, 1-1-1 Kouto, Mikazuki-cho, Sayo-gun, Hyogo 679-5198, Japan, and Department of Applied Physics, Nagoya University, Nagoya 464-8603, Japan

M. Sakata
Department of Applied Physics, Nagoya University, Nagoya 464-8603, Japan

M. Umekawa and N. Hamada
Faculty of Science and Technology, Tokyo University of Science, Chiba 278-8510, Japan

S. Ohkoshi, H. Tokoro, and K. Hashimoto
Research Center for Advanced Science and Technology, University of Tokyo, Tokyo 153-8904, Japan
(Received 29 July 2003; published 17 December 2003)

The charge density distribution has been determined for a transition metal cyanide, $RbMn[Fe(CN)_6]$, by means of the maximum entropy–Rietveld method combined with the highly angularly resolved synchrotron radiation x-ray powder diffraction at SPring-8 BL02B2. We directly observed a charge transfer from the Mn site to the Fe site in the low-temperature phase. On the basis of a local density approximation calculation, we discuss the origin for the anisotropic bonding electron distribution around the Mn^{3+} ion in the low-temperature phase.

DOI: 10.1103/PhysRevLett.91.255502 PACS numbers: 61.10.Nz, 71.27.+a, 78.20.Ls

Transition metal cyanides, $A(\mathrm{I})M(\mathrm{II})[N(\mathrm{III})(\mathrm{CN})_6]$ (A = Na, K, Rb, Cs; M = Mn, Co, Cr; N = Fe, Cr) [1–4], have been attracting the renewed interest of materials scientists, because they show a novel photoinduced magnetization/demagnetization in addition to the thermally induced spin-state transition. For example, Sato *et al.* [3] reported the enhancement of magnetization in $K_{0.2}Co_{1.4}Fe(CN)_6 \cdot 6.9H_2O$ by red light irradiation at 5 K and suppression of magnetization by blue light irradiation at 5 K. In addition to the attracting optomagnetic properties, the transition metal cyanides have the characteristic structure: the transition metal ions are surrounded by six cyanos (CN^-) and form a three-dimensional—M-NC-N—network analogous to the double-perovskite-type transition metal oxides. In this sense, the study of the transition metal cyanides will contribute to deeper comprehension of the strongly correlated electron system. Most of the transition metal cyanides, however, contain considerable nonstoichiometric H_2O molecules, which make the structural analysis difficult.

Among the transition metal cyanides, $RbMn[Fe(CN)_6]$ [5] does not contain extra H_2O molecules and is suitable for precise structural analysis on the charge density level. Ohkoshi *et al.* [5] observed temperature-induced cubic ($F\bar{4}3m$: $Z = 4$) tetragonal ($I\bar{4}m2$; $Z = 2$) transition at around 220 K. The structural transition is ascribed to the charge transfer from the Mn^{2+} site to the Fe^{3+} site, because resultant Jahn-Teller distortion of Mn^{3+} (d^4) can cause the tetragonal structure [6]. With further decrease of temperature below 12 K (= T_C), the local spins at the Mn sites are ferromagnetically ordered, as confirmed by neutron powder diffraction experiment [7]. Tokoro *et al.* [8] observed suppression of magnetization by a visible pulse laser irradiation at 3 K.

In this Letter, we report experimentally determined charge density distribution of $RbMn[Fe(CN)_6]$ and the charge transfer from the Mn site to the Fe site at the cubic-tetragonal transition. In the tetragonal phase, the minimum of the charge density in the in-plane Mn-N_{xy} bond is higher than that of the out-of-plane Mn-N_z bond. At a glance, this charge density is curious because the $d_{x^2-y^2}$ orbital, which expands toward the in-plane nitrogens, should be vacant due to the Jahn-Teller type distortion. We ascribed the charge density on the Mn-N_{xy} bond to the bonding electrons at ≈ -8.0 eV, since the $p_{x(y)} - d_{x^2-y^2}$ hybridization is stronger than the $p_z - d_{3z^2-r^2}$ hybridization.

$RbMn[Fe(CN)_6]$ was prepared by reacting an aqueous solution (0.1 mol dm^{-3}) of $MnCl_2$ with a mixed aqueous solution of RbCl (1 mol dm^{-3}) and $K_3[Fe(CN)_6]$

($0.1\ \mathrm{mol\,dm^{-3}}$) to yield a light brown precipitate [5]. To obtain x-ray powder data of good counting statistics with high angular resolution, measurements were carried out at the SPring-8 BL02B2 beam line [9]. The as-grown sample powders were sealed in a 0.3 mmϕ Lindemann capillary, which gave a homogeneous intensity distribution in the Debye-Scherrer powder ring. The wavelength of the incident x ray was 0.82 Å (nearly over the K edge of Rb), and the exposure time was for 26 min at 300 K and for 67 min at 92 K.

We listed in Tables I and II the results of the Rietveld refinement. The diffraction pattern at 92 K was analyzed by the two-phase model (two $I\bar{4}m2$ phases) [10]. The isotropic atomic displacement parameters B at 92 K are smaller than those at 300 K. One may notice that the Fe-C bond distance [$=1.917(7)$ Å] in the cubic phase is longer than the average [$=1.859(5)$ Å] in the tetragonal phase. This observation is curious since the ionic radius of Fe^{2+} is larger than that of Fe^{3+}. This unexpected behavior is perhaps ascribed to the variation of the bonding electron distribution (see Fig. 3) as well as the significant reduction ($\approx 10.2\%$) of the cell volume at the cubic-tetragonal transition. Here we refer to the fact that the Fe-C bond distance in $Na_{0.42}Co[Fe(CN)_6]_{0.78} \cdot 4.64H_2O$ shows a similar behavior at the charge-transfer transition [11].

The electron density distributions at both temperatures were visualized by the maximum entropy method (MEM [12,13]) combined with the Rietveld refinement. The method has successfully applied to the structural studies of fullerene compounds [14,15], intermetallic compounds, transition metal oxides [16], and so on. The detail of the MEM/Rietveld method is described in previous papers [14,15]. The number of structural factors derived by the Rietveld analysis were 78 (162) at 300 K (at 92 K): the maximum (minimum) d values were 6.10 Å (0.85 Å) at 300 K and 5.88 Å (0.85 Å) at 92 K. The MEM analysis was carried out with a program ENIGMA [17] using $100 \times 100 \times 100$ pixels ($72 \times 72 \times 108$ pixels) at 300 K (at 92 K). In MEM imaging, any kind of deformation of charge density is allowed as long as it satisfies the symmetry requirements. The R_F factors based on the MEM charge densities are 2.1% and 2.9% at 300 and 92 K, respectively.

In Fig. 1, the MEM charge density of the (100) section containing Mn, Fe, C, and N atoms is shown at 300 K with schematics of crystal structure. The contour lines are drawn only for the lower density region ($4.0e\text{Å}^{-3}$). The MEM charge density clearly exhibits the Mn-N and the Fe-C bonding features. The charge density distribution is isotropic around Mn^{2+} because both the e_g orbitals, that is, $d_{x^2-y^2}$ and $d_{3z^2-r^2}$, are occupied in the cubic phase. The minimum of the charge density ($=0.80e\text{Å}^{-3}$) in the Fe-C bond is larger than that ($=0.60e\text{Å}^{-3}$) in the Mn-N bond. This bonding electron distribution is consistent with the picture that $RbMn[Fe(CN)_6]$ consists of $Fe(CN)_6$ complexes and cations (Rb^+ and Mn^{2+}). The charge density distribution drastically changes at the cubic-tetragonal transition. Figure 2(a) shows MEM charge density of $RbMn[Fe(CN)_6]$ for the (110) section at 92 K. One may notice that the charge density distribution around Mn becomes anisotropic: the minimum of the charge density ($=0.65e\text{Å}^{-3}$) in the Mn-N_{xy} bond is higher than that ($=0.28e\text{Å}^{-3}$) in the Mn-N_z bond. Obviously, this anisotropy is ascribed to the charge transfer from the Mn^{2+} site to the Fe^{3+} site, which causes a hole on the e_g orbital of the Mn ion. This charge density, however, is curious because the $d_{x^2-y^2}$ orbital should be vacant due to the Jahn-Teller type distortion (*vide infra*).

Here let us investigate variation of the charge density around the Mn ion and the Fe ion at the cubic-tetragonal transition. Figure 3 shows the charge density of $RbMn[Fe(CN)_6]$ along the Mn-NC-Fe bond at 300 and 92 K. The charge density around the Mn ion significantly decreases in the tetragonal phase. We estimated the total charges around the Mn ion by spherical integration up to the midpoint of the Mn-N bond, i.e., 1.09 Å for the cubic phase and 1.06 Å for the tetragonal phase [18]. The total charge decreases from $23.0(2)e$ to $22.2(2)e$ at the cubic-tetragonal transition, indicating the valence change from Mn^{2+} to Mn^{3+}. The charge density around the Fe ion,

TABLE I. Atomic coordinates, isotropic atomic displacement parameters B, and occupancy g for $RbMn[Fe(CN)_6]$ at 300 K. The space group is $F\bar{4}3m$ ($Z = 4$). Lattice constant is $a = 10.563\,25(3)$ Å. R_{wp}, R_I, and R_e are 8.7%, 3.9%, and 5.7%, respectively.

Atom	Site	g	x	y	z	B (Å^2)
Mn	4a	1	0	0	0	1.00(2)
Fe	4b	1	1/2	1/2	1/2	1.00(2)
Rb1	4c	0.919(1)	1/4	1/4	1/4	8.63(6)
Rb2	4d	0.081(1)	3/4	3/4	3/4	8.63(6)
N	24f	1	0.2068(3)	0	0	2.33(5)
C	24f	1	0.3185(7)	0	0	2.33(5)

TABLE II. Atomic coordinates, isotropic atomic displacement parameters B, and occupancy g for $RbMn[Fe(CN)_6]$ at 92 K. The space group is $I\bar{4}m2$ ($Z = 2$). Lattice constants are $a = 7.087\,37(4)$ Å and $c = 10.5334(1)$ Å. B for C_z, C_{xy}, N_z, and N_{xy} are fixed. R_{wp}, R_I, and R_e are 5.2%, 3.8%, and 3.4%, respectively.

Atom	Site	g	x	y	z	B (Å^2)
Fe	2a	1	0	0	0	0.25(2)
Mn	2b	1	0	0	1/2	0.25(2)
Rb1	2c	0.955(1)	0	1/2	1/4	2.24(4)
Rb2	2d	0.045(1)	0	1/2	3/4	2.24(4)
C_z	4e	1	0	0	0.1738(6)	0.60
C_{xy}	8g	1	0.1882(4)	0.1882(4)	0	0.60
N_z	4e	1	0	0	0.2847(6)	0.60
N_{xy}	8g	1	0.3014(9)	0.3014(9)	0	0.60

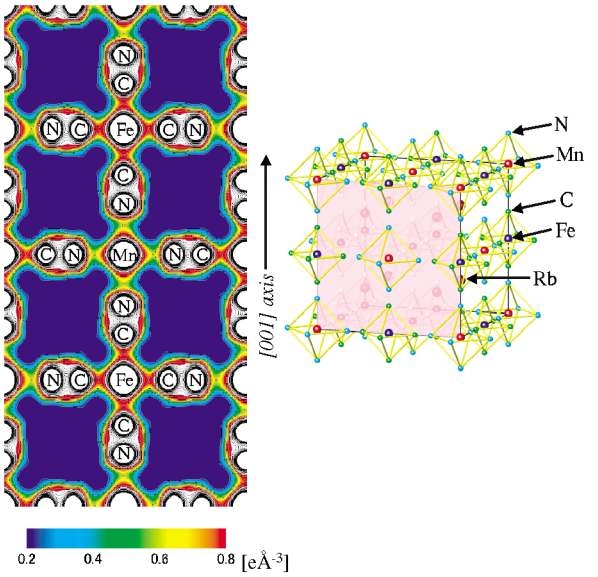

FIG. 1 (color). MEM electron density distribution of $RbMn[Fe(CN)_6]$ for the (100) section at 300 K in the high-temperature ($F\bar{4}3m$: $Z = 4$) cubic phase. Contour lines are drawn from 0.0 to $4.0e$Å^{-3} at intervals of $0.2e$Å^{-3}. Schematics show the crystal structure.

however, scarcely changes at the cubic-tetragonal transition: the total charges rather decreases from $22.9(2)e$ to $22.4(2)e$ at the transition. This unexpected behavior suggests that the transferred electron spreads over the CN^- ligands of the $Fe(CN)_6$ complex.

We have calculated the charge density distribution with the full-potential linearized augmented plane-wave method [19,20] within the local density approximation (LDA) scheme [21–23]. The actual tetragonal lattice parameters (see Table II) at 92 K determined by Rietveld analysis were used. The plane-wave cutoff energies are 15 Ry for the wave function and 60 Ry for the potential and the charge density. We have performed the self-consistence calculation with 288 k points in the irreducible Brillouin zone for the tetragonal lattice. The calculated spin moment μ_{Mn} at the Mn site ($=3.2\mu_B$) is nearly consistent with the experimental results [$\mu_{Mn} = 3.2(7)\mu_B$ [7]]. Figure 2(b) shows the calculated charge density of $RbMn[Fe(CN)_6]$ for the (110) section. Heights and interval of the contour lines are the same for both the experimental [Fig. 2(a)] and calculated [Fig. 2(b)] images. The LDA calculation quantitatively reproduces MEM charge density, including the anisotropic charge density around Mn^{3+}. Actually, the calculated minima of the charge densities are $0.59e$Å^{-3} and $0.32e$Å^{-3} in the Mn-N_{xy} and Mn-N_z bonds, respectively, which are close to the experimentally obtained values ($0.65e$Å^{-3} and $0.28e$Å^{-3} in the Mn-N_{xy} and Mn-N_z bonds, respectively).

Now let us consider the origin for the anisotropic charge density around the Mn^{3+} ion. We show in Fig. 4 partial density of state (DOS) for [Fig. 4(a)] up-spin and [Fig. 4(b)] down-spin electrons. In the up-spin DOS [Fig. 4(a)], four e_g-dominated bands are observed, reflecting strong hybridization of the e_g state with the $2p$ state of the neighboring nitrogens: the lower-lying two bands (≈ -8.0 and ≈ -7.0 eV) and upper-lying two bands (≈ -0.5 and ≈ 0.5 eV) correspond to the bonding and antibonding orbitals made by the e_g ($d_{x^2-y^2}$ and $d_{3z^2-r^2}$) orbitals and the p [$p_{x(y)}$ and p_z] orbitals of the neighboring nitrogens. [The splitting (≈ 1.0 eV) of the e_g levels of Mn^{3+} seems smaller as compared with the Mn^{3+} fluorides [24,25].] Here we emphasize that the energy splitting between the bonding and antibonding orbitals is larger for the Mn-N_{xy} bond, indicating that

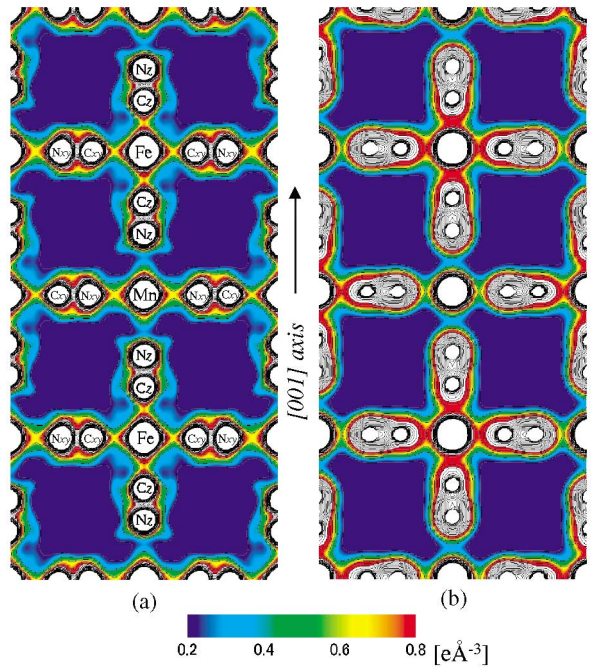

FIG. 2 (color). (a) MEM electron density distribution of $RbMn[Fe(CN)_6]$ for the (110) section in the low-temperature tetragonal ($I\bar{4}m2$; $Z = 2$) phase at 92 K. (b) Electron density distribution of $RbMn[Fe(CN)_6]$ for the (110) section determined by the LDA first principles calculation based on the actual atomic coordinates (see text). Contour lines are drawn from 0.0 to $4.0e$Å^{-3} at intervals of $0.2e$Å^{-3}.

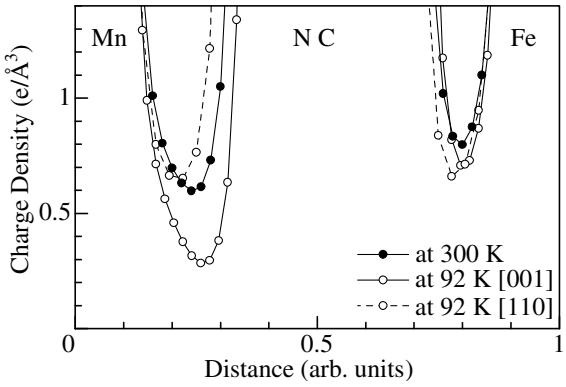

FIG. 3. Charge density of $RbMn[Fe(CN)_6]$ along the Mn-NC-Fe bond at 300 and 92 K, determined by MEM/Rietveld analysis.

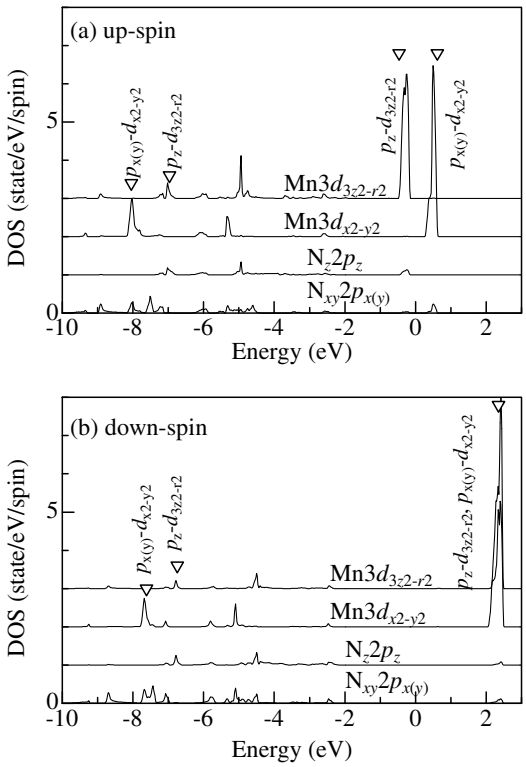

FIG. 4. Partial density of state (DOS) for (a) up-spin and (b) down-spin electrons. N_z and N_{xy} represent the apical and in-plane nitrogens, respectively.

the $p_{x(y)} - d_{x^2-y^2}$ hybridization is stronger than the $p_z - d_{3z^2-r^2}$ hybridization. If the charge density on the Mn-N bonds originates in the bonding electrons, the value is larger in the Mn-N_{xy} bond, as is observed in Figs. 2(a) and 2(b). This argument suggests that the anisotropic charge density around the Mn^{3+} ion can be ascribed to the bonding electrons at ≈ -8.0 eV below the Fermi level E_F, not to the bare e_g electrons near E_F.

The most important factor for the stronger $p_{x(y)} - d_{x^2-y^2}$ hybridization is, of course, the shorter Mn-N_{xy} bond distance [= 1.991(9) Å] due to the Jahn-Teller distortion of the MnN_6 octahedron. Another factor may be the occupancy for the up-spin $d_{x^2-y^2}$ orbitals (=0.31), because the atomic orbital whose occupancy is close to 1/2 mainly contributes to the chemical bonding. This electronic situation further stabilizes the bonding orbital and enhances the anisotropic charge density around Mn^{3+}. These arguments suggest that the $p - d$ hybridization plays a significant role even in the Jahn-Teller instability.

In summary, we have investigated variation of charge density at the Jahn-Teller transition of RbMn[$Fe(CN)_6$] and directly observed the charge transfer from the Mn site to the Fe site at the cubic-tetragonal transition. We further interpreted the anisotropic charge density distribution around Mn^{3+} in terms of the bonding electrons. Thus, the MEM/Rietveld charge density analysis is proved to be effective for deeper comprehension of the transition metal compounds.

This work was supported by a Grant-In-Aid for Scientific Research from the Ministry of Education, Culture, Sports, Science and Technology and Yazaki Foundation. The synchrotron radiation x-ray powder diffraction experiments were performed at the SPring-8 BL02B2 beam line with approval of the Japan Synchrotron Radiation Research Institute (JASRI).

[1] T. Mallah *et al.*, Science **262**, 1554 (1993).
[2] O. Sato *et al.*, Science **271**, 49 (1996).
[3] O. Sato *et al.*, Science **272**, 704 (1996).
[4] S. Ferlay *et al.*, Nature (London) **378**, 701 (1995).
[5] S. Ohkoshi *et al.*, J. Phys. Chem. B **106**, 2423 (2002).
[6] Y. Moritomo *et al.*, J. Phys. Soc. Jpn. **71**, 2078 (2002).
[7] Y. Moritomo *et al.*, J. Phys. Soc. Jpn. **72**, 456 (2003).
[8] H. Tokoro, S. Ohkoshi, and K. Hashimoto, Appl. Phys. Lett. **82**, 1245 (2003).
[9] E. Nishibori *et al.*, Nucl. Instrum. Methods Phys. Res., Sect. A **467–468**, 1045 (2001).
[10] There exist discrepancies of the atomic coordinates between the present work and Ref. [6] for both the cubic and tetragonal phases. The structural solution reported in Ref. [6] for the cubic phase was trapped at a wrong local minimum. The slight discrepancy of the tetragonal structure is due to the different structural model: the two-phase model was adopted in the present work, while the single-phase model was adopted in Ref. [6].
[11] M. Hanawa *et al.*, J. Phys. Soc. Jpn. **72**, 987 (2003).
[12] M. Sakata and M. Sato, Acta Crystallogr. Sect. A **A46**, 263 (1990).
[13] M. Takata and M. Sakata, Acta Crystallogr. Sect. A **A52**, 287 (1996).
[14] M. Takata *et al.*, Nature (London) **377**, 46 (1995).
[15] M. Takata *et al.*, Phys. Rev. Lett. **78**, 3330 (1997).
[16] M. Takata *et al.*, J. Phys. Soc. Jpn. **68**, 2190 (1999).
[17] H. Tanaka *et al.*, J. Appl. Crystallogr. **35**, 282 (2002).
[18] The total charge of the Mn ion becomes 23.9(2)e [23.1(2)e] for the high-temperature (low-temperature) phase if we integrate the charge density up to the minimum in the Mn-N bond.
[19] O. K. Andersen, Phys. Rev. B **12**, 3060 (1975).
[20] T. Takeda and J. Kubler, J. Phys. F: Met. Phys. **9**, 661 (1979).
[21] P. Hohenberg and W. Kohn, Phys. Rev. **136**, B864 (1964).
[22] W. Kohn and L. J. Sham, Phys. Rev. **140**, A1133 (1965).
[23] S. H. Vosko, L. Wilk, and M. Nusair, Can. J. Phys. **58**, 1200 (1980).
[24] F. Rodriguez and F. Aguado, J. Chem. Phys. **118**, 10 867 (2003).
[25] The discrepancies of the splitting of the e_g levels of Mn^{3+} are partly due to the limitation of the LDA calculation and partly due to the unoccupied molecular orbitals of CN^-, because not only the σ state located at ~ -8 eV but also the σ^* state at ~ 10 eV hybridizes with the e_g orbitals of Mn^{3+} and affects the magnitude of the splitting of the levels.